Combined experimental and *ab initio* study of the electronic structure of narrow-diameter single-wall carbon nanotubes with predominant (6,4),(6,5) chirality

K. De Blauwe,[1] D. J. Mowbray,[2,3] Y. Miyata,[4] P. Ayala,[1] H. Shiozawa,[5] A. Rubio,[2,3,6] P. Hoffmann,[7] H. Kataura,[8,9] and T. Pichler[1]

[1]*Faculty of Physics, University of Vienna, Strudlhofgasse 4, A-1090 Vienna, Austria*

[2]*Nano-Bio Spectroscopy group and ETSF Scientific Development Centre, Depto. Física de Materiales, Universidad del País Vasco, Av. Tolosa 72, E-20018 San Sebastián, Spain*

[3]*Centro de Física de Materiales, DIPC, CSIC-UPV/EHU-MPC, Av. Tolosa 72, E-20018 San Sebastián, Spain*

[4]*Department of Chemistry, Nagoya University, Furo-cho, Chikusa-ku, Nagoya 464-8602, Japan*

[5]*Advanced Technology Institute, University of Surrey, Guildford GU2 7XH, United Kingdom*

[6]*Fritz-Haber-Institut der Max-Planck-Gesellschaft, Berlin, Germany*

[7]*BESSY II, Helmholtzcenter Berlin, D-12489 Berlin, Germany*

[8]*Nanosystem Research Institute, AIST, Tsukuba 305-8562, Japan*

[9]*CREST, JST, Tsukuba 305-8562, Japan*

(Received 25 June 2010; revised manuscript received 19 August 2010; published 24 September 2010)

Narrow diameter tubes and especially (6,5) tubes with a diameter of 0.75 nm are currently one of the most studied carbon nanotubes because their unique optical and especially luminescence response makes them exceptionally suited for biomedical applications. Here we report on a detailed analysis of the electronic structure of nanotubes with (6,5) and (6,4) chiralities using a combined experimental and theoretical approach. From high-energy spectroscopy involving x-ray absorption and photoemission spectroscopy the detailed valence- and conduction-band response of these narrow diameter tubes is studied. The observed electronic structure is in sound agreement with state of the art *ab initio* calculations using density-functional theory.

DOI: 10.1103/PhysRevB.82.125444 PACS number(s): 71.20.Tx, 71.10.Hf, 73.63.Fg

I. INTRODUCTION

In recent years there has been tremendous progress in obtaining a sound understanding of the mechanical, electronic, and optical properties of single-wall carbon nanotubes (SWCNTs).[1] Specifically, narrow diameter tubes and especially (6,5) tubes with a diameter of 0.75 nm are currently one of the most studied SWCNTs. This is because of their exceptional enrichment established in the CoMoCAT synthesis process[2] and their unique optical and especially luminescence response.[3] They have the special property of fluorescing in a region of the near infrared,[4] where human tissue and biological fluids are particularly transparent for their emission. This makes them very useful for biological imaging as well as for biosensing.[5–7] Surprisingly, much less is known on the direct experimental and *ab initio* theoretical analysis of their electronic structure which is crucial for understanding their optical response.

Different methods have been developed and optimized to synthesize such small diameter tubes below 0.8 nm diameter and especially with (6,5) and (6,4) chiralities. Kitiyanan *et al.*[2] successfully controlled the production of SWCNTs by catalytic decomposition of CO on bimetallic Co-Mo catalysts yielding an enrichment of (6,5) tubes. On the other hand, a pattern of (6,5) and (6,4) tubes have been successfully synthesized via nanochemical reaction inside SWCNTs,[8] i.e., the growth of double-wall carbon nanotubes. This was successfully achieved by high-temperature annealing of peapods (C_{60} @ SWCNTs) without any further catalyst[9–11] and by a catalytic reaction in metallocene filled SWCNTs.[12–14] Besides this direct growth of narrow diameter tubes, in recent years great progress in the separation of narrow diameter tubes has been achieved.[15–21] The main techniques comprise DNA wrapping,[15,18,22,23] chromatographic separation,[15,19] and density gradient ultracentrifugation (DGU).[20] It is also possible to enrich the SWCNTs sample in mainly one (n,m) tube type. In particular, (6,5) SWCNTs have been both separated successfully[15–18] and analyzed regarding their photoluminescence response. However, for most of these samples the direct observation of their electronic properties by surface-science techniques was complicated by the presence of byproducts from the used surfactant and/or by the low yield of the separation process. Only very recently purified samples without remaining surfactant of (6,4),(6,5) chirality enrichment, have been available as bulk mats of SWCNTs (a so-called buckypaper).[21]

Concomitant to the synthesis and optical characterization, several theoretical approaches have been used to analyze the electronic structure and the optical response of narrow diameter tubes. For these tubes, semi-empirical tight-binding (TB) calculations, which work very well for large diameter SWCNTs,[1,24] have to be extended since they neglect curvature effects in their description of the electronic structure. Particularly for small diameter tubes, the carbon-carbon bonds on the curved nanotube surface become inequivalent as π orbitals, being parallel in graphite, are no longer parallel on a curved surface. This involves a change in overlap between neighboring π orbitals. This was partly solved by Popov[25] who studied the effect of curvature on the structure, electronic, and optical properties of isolated SWCNTs within a symmetry-adapted nonorthogonal tight-binding model using $2s$ and $2p$ electrons of carbon. However, the exact values for the transition energies are still not reproduced sufficiently well.

Ab initio calculations of highly chiral small diameter SWCNTs have until recently been too computationally expensive since the unit cell of the (6,5) and (6,4) tubes contain hundreds of atoms. Hence, to date there is only one result from Chang *et al.*[26] utilizing a symmetry-adapted local-density approximation *ab initio* approach to calculate such tubes with large unit cell. These results were successfully applied to calculate the optical matrix elements and exciton binding energies for (6,5) tubes in comparison to two-photon experiments.[27]

In this paper we report on a detailed analysis of the electronic structure of small diameter nanotubes with enriched (6,4),(6,5) chirality with a combined experimental and theoretical approach. From high-energy spectroscopy involving x-ray absorption spectroscopy (XAS) and photoemission (PES) the detailed valence- and conduction-band response of these narrow diameter tubes is probed. The observed electronic structure is in sound agreement with our extensive state of the art *ab initio* density-functional theory (DFT) calculations using the generalized gradient approximation (GGA).

II. METHODS

The experiments are carried out on a CoMoCAT sample, enriched with (6,5) SWCNTs by DGU method.[21] After filtering, the obtained buckypaper was transferred onto a copper sample holder fixed by a Ta foil and annealed at 1000 K. This was performed in a UHV preparation chamber followed by a subsequent transfer to a variable temperature He cryostat attached to the measurement chamber. The base pressure was always below 2×10^{-10} mbar.

The PES and XAS experiments were performed at beamline UE 52 PGM at Bessy II, which has a resolving power $(E/\Delta E)$ of 4×10^4.[28] For PES a hemispherical photoelectron energy analyzer SCIENTA SES 4000, with the energy resolution set to 10 meV, was used. XAS was conducted in the total electron yield mode. All spectra were recorded at 15 K with an effective energy resolution better than 30 meV. The excitation energies were calibrated by the Fermi edge of clean Au films and the XAS response was normalized to the background absorbance measured on the same Au films.

The enrichment was checked by resonance Raman optical absorption and luminescence spectroscopy taking into account the corresponding different cross sections for the individual tubes. We found that the enrichment of (6,4) and (6,5) tubes, which are roughly of equal concentration in the bulk sample, is about 80% of all thin diameter nanotubes.[29] In this report we also determined the main fractions of the other 20% of tubes which are of (7,5), (8,4), and (9,1) chiralities. For comparison, we also show results on a sample with large diameter semiconducting SWCNTs (SC-SWCNTs) from Ref. 30, with a mean diameter of 1.37 nm.

All calculations have been performed using the real-space DFT code GPAW,[31] based on the projector-augmented wave method with the GGA Perdew-Burke-Ernzerhof (PBE) exchange-correlation functional.[32] A grid spacing of 0.2 Å was used to represent the electron density and wave functions, and all structures were relaxed until a maximum force below 0.03 eV/Å was obtained. For the unit cells obtained upon minimization a Γ-point sampling of the Brillouin zone was sufficient to describe the equilibrium electron density [(6,4) SWNT dimensions: $18.618\times20.0\times20.0$ Å^3, (6,5) SWNT dimensions: $40.747\times20.0\times20.0$ Å^3]. However, to describe the density of states a 50 **k**-point sampling of the Brillouin zone along the nanotube axis was employed with the equilibrium electron density kept fixed.

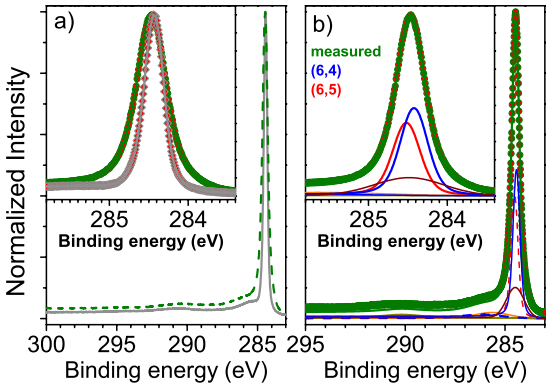

FIG. 1. (Color online) (a) C 1*s* photoemission response of the (6,4),(6,5) enriched sample (outer green curve) in comparison to purely semiconducting SWCNT with 1.37 nm mean diameter from Ref. 30 (gray curve), measured with a photon excitation energy of 400 eV at a temperature of 35 K. The inset shows the C 1*s* line in an expanded scale. (b) Line-shape analysis of the C 1*s* response of the (6,4),(6,5)-enriched buckypaper using Voightian line shapes and a Shirley background. The inset shows the three components [(6,4) as blue curve and (6,5) as red curve] of the C 1*s* line on an expanded scale.

III. RESULTS AND DISCUSSION

We now turn to a detailed discussion of the direct assessment of the electronic structure of the SWCNTs with (6,4) and (6,5) chiralities in comparison to our *ab initio* calculations. As a first check, we determined the sample purity and sample composition in comparison to the results obtained from optical techniques.[29] We used an x-ray photoemission spectroscopy survey scan for checking the purity regarding contamination from adsorbates and remaining surfactants and catalysts. Only very small contamination from oxygen was detected within the limit of 0.5% and no remaining metal catalysts have been observed within the detection limit. Therefore, we can safely state that the purity is higher than 98%.[33]

Regarding the analysis of the sample composition we performed a detailed line-shape analysis of the C 1*s* response, depicted in Fig. 1. The left panel of the figure shows a comparison of the response of the (6,4),(6,5) chirality-enriched sample and the purely semiconducting nanotubes with 1.37 nm mean diameter[30] using an excitation energy of 400 eV. The inset shows the C 1*s* response in an expanded scale. The maximum represents the binding energy and is 284.47 eV for the (6,4),(6,5) enriched sample and 284.43 eV for the semiconducting reference SWCNTs. The binding-energy difference of 40 meV between the maxima highlights that the

binding energy is slightly dependent on diameter and chirality. Both peaks are, as expected, characterized by a symmetric Voigtian line shape with a full width at half maximum of 0.46 eV for the (6,4),(6,5) chirality-enriched sample and 0.29 eV for the thick diameter semiconducting sample.

One explanation for the increased linewidth for the (6,4),(6,5) sample, also in comparison with graphite (0.32 eV), is the larger bond-angle variation for narrow-diameter tubes due to the strong curvature.[34] However, the linewidth is significantly broader than for C_{60}, which has a similar curvature and also only one sp^2 bonding environment. On the other hand, a change in the sp^2 bonding environment is not expected to be curvature dependent and would yield a much more pronounced increase in the linewidth. For instance, even without changing the I_h symmetry of the fullerene cage when going from C_{60} to $Dy_3N@C_{80}$ or $Sc_3N@C_{80}$ (Refs. 35 and 36) the different sp^2 bonding environments in the C_{80} cage results in a C 1*s* linewidth of 0.9 eV. Therefore, we can safely assign the increased linewith in the (6,4),(6,5) chirality-enriched sample to the distribution of different binding energies for these different narrow diameter tubes.

In order to further support this assessment we performed a detailed line-shape analysis of the C 1*s* response using Voigthian lines and a Shirley background including the response from the plasmon satellites and the shake up structures. The results are depicted in the right panel of Fig. 1. We observe a very good agreement using three components for the main C 1*s* line and three broad contributions for the shake up and the π and $\pi+\sigma$ plasmon satellites. The details are depicted in the inset of the right panel of Fig. 1. The three peaks at 284.42, 284.49, and 284.52 eV have a relative spectral weight of 44%, 20%, and 36%, respectively. These results are in sound agreement with the (6,5) to (6,4) ratio of about 1:1 and the 80% enrichment factor of these chiralities determined from our optical experiments.[29] In keeping with the results mentioned below, we assign the binding energy of 284.42 eV to the (6,4) tubes and the higher binding energy of 284.52 eV to the (6,5) tubes. In other words, they have a binding-energy difference of 100 meV. The linewidth of these two components is 0.41 eV. The increased linewidth of about 1 eV of the 284.49 eV component can be related to the mixture of the different narrow diameter tubes with (7,5), (8,2), and (9,1) chiralities as main contributions.

We now turn to a detailed analysis of the valence-band response. In the left panel of Fig. 2 the photoemission spectrum of the valence band, measured with an excitation energy of 150 eV, is plotted for the (6,5)/(6,4) enriched sample (green curve) and the SC-SWCNTs with 1.37 nm mean diameter (gray curve).[30] The overall shape is again very similar but has distinct differences in the line shape close to the Fermi level. In order to analyze the details in the electronic structure of the π bands, we elucidated the valence-band photoemission in a high-resolution closeup at low binding energies. The results are depicted in the right panel of the figure. As expected, the experimental result is dominated by a strong peak which is related to the underlying π maximum in the density of states (DOS) concomitant to the saddle-point singularity at the M point of the graphene parent compound. In addition, a distinct fine structure in the DOS is

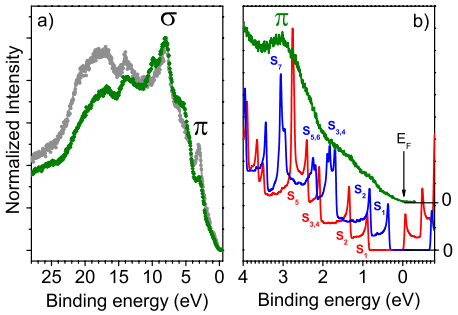

FIG. 2. (Color online) (a) Valence-band photoemission spectrum of the (6,4),(6,5) chirality-enriched sample (green curve) and only semiconducting reference SC-SWCNT (gray curve), measured with photon excitation energy of 150 eV. (b) High-resolution closeup of the (6,4),(6,5) chirality-enriched sample in comparison to *ab initio* calculations of the DOS of (6,4) (blue curve) and (6,5) tubes (red curve). The calculated DOS are shifted against the Fermi level of gold to account for the different chemical potentials. The labels S_1, S_2, $S_{3,4}$, and $S_{5,6}$ correspond to the position of the respective van Hove singularities in the valence band. π indicates the DOS maximum, E_F the Fermi energy.

observed which can be closely matched with previous results on metallicity-mixed[37,38] and metallicity-separated SWCNTs (Ref. 30) with thick diameters assigned to van Hove singularities (vHSs) in the DOS. In our previous results a very good agreement with diameter cumulative tight-binding calculations was observed. As mentioned above, such calculations fail because of strong curvature induced changes in the tight-binding overlap. Therefore we performed state of the art *ab initio* calculations for both the (6,4) (blue curve in the figure) and (6,5) tubes (red curve in the figure) and compared it to the experimental results after applying a Gaussian resolution broadening.

In order to account for the different chemical potentials of the (6,4) and (6,5) tubes in comparison to the reference Fermi level of gold and the strong underestimation of the actual energy gaps in the *ab initio* calculations of up to 0.2 eV we shifted the calculated DOS by +0.18 eV for the (6,4) tubes and by −0.4 eV for the (6,5) tubes, respectively.[39] Although the absolute values of the shift is not the same as for the change in the respective C 1*s* binding energy depicted in Fig. 1, the results explain the higher binding energy of 0.1 eV of the (6,5) tubes. After accounting for this correction, the energy position of the calculated vHs of both tube types correspond very well to the measured peaks in the valence-band response. The peaks in the DOS are indicated by the labels S_1, S_2, $S_{3,4}$, and $S_{5,6}$ for the vHS of the semiconducting (6,5) and (6,4) tubes. Interestingly, for the (6,5) tubes the Fermi level is pinned to the onset of the conduction band whereas for the (6,4) tubes the conduction-band onset it about 0.68 eV above the reference. This difference in the chemical potential might be explained by differences in the contact potential of these very narrow diameter tubes due to their strong curvature.[40]

The first peak at 0.36 eV can be assigned to the corresponding S_1 vHS of the (6,4) tubes, the second peak at 0.84 eV is related to the first vHS S_1 of the (6,5) and the S_2 vHS of the (6,4) tubes. The peak at 1.36 corresponds to the

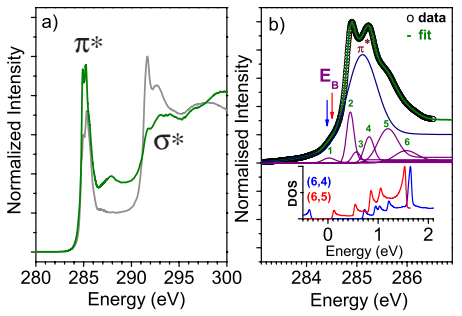

FIG. 3. (Color online) (a) XAS spectrum representing the conduction band of the (6,4),(6,5) chirality-enriched sample (green curve) and only semiconducting reference SC-SWCNT (gray curve). (b) High-resolution close up of the (6,4),(6,5) chirality-enriched sample in an energy range of 2 eV above the C 1*s* edge. The circles represent the measured data. The thick green line is the fit using a broad peak from the π^* response along the colored purple. The C 1*s* binding energy of the (6,4) and (6,5) tubes is highlighted by the arrows. In the inset below the *ab initio* calculated DOS is plotted for the individual (6,5) (red) and (6,4) (blue) SWCNT. As a reference point the binding energy of the (6,4) tubes was used.

S_2 vHS of the (6,5) tubes whereas the broad feature at about 1.9 eV is related to the $S_{3,4}$ vHS of the (6,4) tubes. As the overlap between the higher vHs increases, it is harder to distinguish the individual different vHS related to the broad π peak with a shoulder and a broad hump at a lower binding energy. This hump can be assigned to the $S_{3,4}$ vHS of the (6,5) tubes and the $S_{5,6}$ vHS of the (6,4) tubes, respectively. Interestingly, the shoulder and the main peak can be distinctively assigned to the S_5 vHS of the (6,5) tubes and the S_7 vHS of the (6,4) SWCNT.

We now turn to another independent comparison of the *ab initio* results of the conduction band to the strongly excitonic XAS response. The results are plotted in Fig. 3. The left panel shows an overlay of the (6,5)/(6,4) enriched sample and the previously measured response of only semiconducting tubes. The overall shape is similar in terms of the general features regarding the π^* and the σ^* edges typical for sp^2 carbons. They are characterized by a sharp π^* resonance around 285 eV which is known to be strongly excitonic and downshifted about 2 eV due to the C 1*s* core-hole effect[41–43] and an excitonic σ^* threshold at 291.19 eV.[44] However, there are distinct differences in the fine structure.

Concomitant to our previous results this fine structure is a fingerprint for the one-dimensional band structure of the SWCNT. Therefore, it is strongly depending on the position of the vHS in the different diameter tubes. Interestingly, for the (6,4),(6,5) chirality-enriched sample an additional broad but structured feature is observed at about 288 eV. This feature can be assigned to the response of higher lying vHS of the conduction bands of the (6,5) and (6,4) enriched samples. In contrast to the diameter cumulative response from thick diameter semiconducting tubes these vHSs are well separated and can therefore be easily detected. This is in good agreement with the observation in valence-band photoemission that the S_5 vHS of the (6,5) tubes and the S_7 vHS of the (6,4) SWCNTs are well separated.

In order to analyze the unoccupied DOS in the (6,4),(6,5) chirality-enriched sample in more detail we performed a detailed line-shape analysis in an extended energy range of 2 eV above the π^* onset. The results are depicted in the right panel of Fig. 3. The open black circles represent the measured data points of this C 1*s* edge. The thick green line is the fit using a broad peak from the π^* response along the tube axis (dark blue line) and a fine structure of six Gaussian peaks labeled by the numbers. These are colored purple. The C 1*s* binding energy of the (6,4) and (6,5) tubes is highlighted by the arrow. In the inset below the *ab initio* calculated DOS is plotted for the individual (6,5) (red) and (6,4) (blue) SWCNT. As a reference point the binding energy of the (6,4) tubes was used. The broad π^* resonance has a maximum at 285.16 eV. The six smaller peaks are observed at 284.45 eV, 284.86 eV, 284.99 eV, 285.24 eV, 285.61 eV, and 285.99 eV, respectively.

In the *ab initio* calculated DOS for the individual (6,5) and (6,4) tubes the (6,5) DOS is referenced to the binding energy of the (6,4) tubes and hence shifted by 0.1 eV according to the binding-energy difference. This is a fully self-consistent description taking into account the differences in their respective chemical potentials.

The twofold response consisting of a strongly excitonic π^* resonance from the delocalized states along the tube axis and the weakly modified response from the vHS polarized perpendicular to the tube axis is obvious and in good agreement to our previous results on thick-diameter tubes.[30,42] The energy positions are also well reproduced with the relative intensities modified by core hole effects. The calculated energy difference between the first and second vHSs and second and third vHSs of the unoccupied DOS amount to 0.43 and 0.31 eV for the (6,5) and 0.22 and 0.09 eV for the (6,4) tubes. The difference between the third and fourth vHSs and between the fourth and fifth vHSs is 0.29 and 0.48 eV for the (6,5) tubes and 0.18 and 0.42 eV for the (6,4) tubes. Comparing the observed six peaks from the line-shape analysis with the response from the vHS in the DOS, the first two peaks can be safely assigned to the S_1^* and S_2^* vHSs of the (6,5) tubes in the conduction band, respectively. The third peak, labeled number 3 is assigned to the S_1^* vHS of the (6,4) tubes whereas peak numbers 4 and 5 can be deconvoluted into a superposition of the response from the $S_{3,4}^*$ and $S_{2,3,4}^*$ vHSs of the (6,5) and (6,4) nanotubes, respectively. Finally, the last peak number six is a superposition of their respective S_5^* vHS. The agreement in the relative energy positions is very good and further supports our self-consistent description of the electronic structure of (6,4) and (6,5) SWCNTs.

IV. SUMMARY

We performed a detailed experimental and theoretical study on the electronic structure of the valence and conduction bands of (6,5) and (6,4) nanotubes. We find a sound agreement between the calculated relative energy positions of the vHS in the DOS of our *ab initio* calculations and the measured DOS of the conduction- and valence-band

response as directly measured by high-resolution photoemission and x-ray absorption. The relative ratio of the different SWCNTs in our buckypaper is verified by a line-shape analysis of the C 1*s* photoemission response. The chemical potential between the (6,5) nanotubes and the even narrower (6,4) tubes differs by about 0.7 eV. This might be explained by the different interactions induced by the increased curvature.

Our results set the solid basis for the electronic structure of these narrow diameter tubes and pave the way to a detailed understanding of their electronic and optoelectronic applications as well as for understanding their optical response in nanomedicine and nanobiology.

ACKNOWLEDGMENTS

K.D.B., P.A., and T.P. acknowledge support from the DFG under Projects No. PI 440 3/4/5 and the No. FWF P21333-N20 and the EU for travel support at the beamtime at BESSY II. D.J.M. and A.R acknowledge funding by Spanish MEC (Grant No. FIS2007-65702-C02-01), "Grupos Consolidados UPV/EHU del Gobierno Vasco" (Grant No. IT-319-07), ACI-Promociona (Grant No. ACI2009-1036), and ETSF-I3 (Contract No. 211956). Y.M. acknowledges the financial support by a Grant-in-Aid for Young Scientists (Start-up) from the Japan Society for the Promotion of Science. H.S. acknowledges support from the Leverhulme Trust.

[1] R. Saito, G. Dresselhaus, and M. Dresselhaus, *Physical Properties of Carbon Nanotubes* (Imperial College Press, London, 1998).
[2] B. Kitiyanan, W. E. Alvarez, J. H. Harwell, and D. E. Resasco, Chem. Phys. Lett. **317**, 497 (2000).
[3] S. M. Bachilo, M. S. Strano, C. Kittrell, R. H. Hauge, R. E. Smalley, and R. B. Weisman, Science **298**, 2361 (2002).
[4] M. J. O'Connell *et al.*, Science **297**, 593 (2002).
[5] P. W. Barone, S. Baik, D. A. Heller, and M. S. Strano, Nature Mater. **4**, 86 (2005).
[6] D. A. Heller *et al.*, Nat. Nanotechnol. **4**, 114 (2009).
[7] Z. Liu, S. Tabakman, K. Welsher, and H. J. Dai, Nano Res. **2**, 85 (2009).
[8] R. Pfeiffer, T. Pichler, Y. A. Kim, and H. Kuzmany, Carbon Nanotubes **111**, 495 (2008).
[9] S. Bandow, M. Takizawa, K. Hirahara, M. Yudasaka, and S. Iijima, Chem. Phys. Lett. **337**, 48 (2001).
[10] R. Pfeiffer, F. Simon, H. Kuzmany, and V. N. Popov, Phys. Rev. B **72**, 161404 (2005).
[11] R. Pfeiffer, H. Kuzmany, C. Kramberger, C. Schaman, T. Pichler, H. Kataura, Y. Achiba, J. Kurti, and V. Zolyomi, Phys. Rev. Lett. **90**, 225501 (2003).
[12] H. Shiozawa, T. Pichler, A. Gruneis, R. Pfeiffer, H. Kuzmany, Z. Liu, K. Suenaga, and H. Kataura, Adv. Mater. **20**, 1443 (2008).
[13] H. Shiozawa *et al.*, Phys. Rev. B **77**, 153402 (2008).
[14] H. Shiozawa, T. Pichler, C. Kramberger, M. Rummeli, D. Batchelor, Z. Liu, K. Suenaga, H. Kataura, and S. R. P. Silva, Phys. Rev. Lett. **102**, 046804 (2009).
[15] X. L. Li, X. M. Tu, S. Zaric, K. Welsher, W. S. Seo, W. Zhao, and H. J. Dai, J. Am. Chem. Soc. **129**, 15770 (2007).
[16] Y. H. Miyauchi, S. H. Chiashi, Y. Murakami, Y. Hayashida, and S. Maruyama, Chem. Phys. Lett. **387**, 198 (2004).
[17] Y. Miyauchi, R. Saito, K. Sato, Y. Ohno, S. Iwasaki, T. Mizutani, J. Jiang, and S. Maruyama, Chem. Phys. Lett. **442**, 394 (2007).
[18] M. Zheng, A. Jagota, E. D. Semke, B. A. Diner, R. S. Mclean, S. R. Lustig, R. E. Richardson, and N. G. Tassi, Nature Mater. **2**, 338 (2003).
[19] J. A. Fagan, J. R. Simpson, B. J. Bauer, S. H. D. Lacerda, M. L. Becker, J. Chun, K. B. Migler, A. R. H. Walker, and E. K. Hobbie, J. Am. Chem. Soc. **129**, 10607 (2007).
[20] M. S. Arnold, A. A. Green, J. F. Hulvat, S. I. Stupp, and M. C. Hersam, Nat. Nanotechnol. **1**, 60 (2006).
[21] Y. Miyata, K. Yanagi, Y. Maniwa, T. Tanaka, and H. Kataura, J. Phys. Chem. C **112**, 15997 (2008).
[22] M. Zheng *et al.*, Science **302**, 1545 (2003).
[23] X. M. Tu, S. Manohar, A. Jagota, and M. Zheng, Nature (London) **460**, 250 (2009).
[24] S. Reich, C. Thomsen, and J. Maultzsch, *Carbon Nanotubes: Basic Concepts and Physical Properties* (Wiley-VCH, Weinheim, Germany, 2004).
[25] V. N. Popov, New J. Phys. **6**, 17 (2004).
[26] E. Chang, G. Bussi, A. Ruini, and E. Molinari, Phys. Rev. Lett. **92**, 196401 (2004).
[27] J. Maultzsch, R. Pomraenke, S. Reich, E. Chang, D. Prezzi, A. Ruini, E. Molinari, M. S. Strano, C. Thomsen, and C. Lienau, Phys. Rev. B **72**, 241402 (2005).
[28] A. Scholl, Y. Zou, T. Schmidt, R. Fink, and E. Umbach, J. Electron Spectrosc. Relat. Phenom. **129**, 1 (2003).
[29] F. Simon, K. De Blauwe, Y. Miyata, H. Kataura, D. Mowbray, A. Rubio, H. Kuzmany, and T. Pichler (unpublished).
[30] P. Ayala *et al.*, Phys. Rev. B **80**, 205427 (2009).
[31] J. J. Mortensen, L. B. Hansen, and K. W. Jacobsen, Phys. Rev. B **71**, 035109 (2005).
[32] J. P. Perdew, K. Burke, and M. Ernzerhof, Phys. Rev. Lett. **77**, 3865 (1996).
[33] K. De Blauwe, Y. Miyata, P. Ayala, H. Kataura, D. Mowbray, A. Rubio, P. Hoffman, and T. Pichler (unpublished).
[34] J. Kürti, V. Zólyomi, M. Kertesz, and G. Y. Sun, New J. Phys. **5**, 125 (2003).
[35] L. Alvarez *et al.*, Phys. Rev. B **66**, 035107 (2002).
[36] H. Shiozawa *et al.*, Phys. Rev. B **72**, 195409 (2005).
[37] H. Ishii *et al.*, Nature (London) **426**, 540 (2003).
[38] H. Rauf, T. Pichler, M. Knupfer, J. Fink, and H. Kataura, Phys. Rev. Lett. **93**, 096805 (2004).
[39] We performed symmetry adapted third-next-nearest-neighbor TB calculations based on GW calculations for graphite (Ref. 45) which showed that the energy gap of our DFT calculations is indeed underestimated by about 0.2 eV. However, this fit works only in the vicinity of the Fermi level. A simple upscaling of the energy scale by 16% reproduces the energy gap but fails in the description of the high-energy vHS. This again points to the importance of the inclusion of curvature effects in the description of these narrow diameter tubes and explains the good agreement of our DFT calculations regarding the relative separations of the vHS in the SWCNTs DOS.

[40] Since we performed our measurements on a buckypaper the actual contact potential is determined by the contact between the individual SWCNTs and the copper sample holder. In our recent doping-dependent experiments on buckypaper of SWCNTs with mixed metallicity we observed that the actual contact potential of the metallic and semiconducting SWCNTs is different (Ref. 46). Therefore, it is in very good agreement with this previous observation that the (6,4) and (6,5) with different and very high curvature have different contact potential with respect to the copper sample holder.

[41] P. A. Brühwiler, P. Kuiper, O. Eriksson, R. Ahuja, and S. Svensson, Phys. Rev. Lett. **76**, 1761 (1996).

[42] C. Kramberger, H. Rauf, H. Shiozawa, M. Knupfer, B. Buchner, T. Pichler, D. Batchelor, and H. Kataura, Phys. Rev. B **75**, 235437 (2007).

[43] E. L. Shirley, Phys. Rev. Lett. **80**, 794 (1998).

[44] E. J. Mele and J. J. Ritsko, Phys. Rev. Lett. **43**, 68 (1979).

[45] A. Grüneis, C. Attaccalite, L. Wirtz, H. Shiozawa, R. Saito, T. Pichler, and A. Rubio, Phys. Rev. B **78**, 205425 (2008).

[46] C. Kramberger, H. Rauf, M. Knupfer, H. Shiozawa, D. Batchelor, A. Rubio, H. Kataura, and T. Pichler, Phys. Rev. B **79**, 195442 (2009).